



HAL
open science

Relative abundances of methane- and sulfur-oxidizing symbionts in gills of the deep-sea hydrothermal vent mussel *Bathymodiolus azoricus* under pressure

Kamil M. Szafranski, Bérénice Piquet, Bruce Shillito, François Lallier,
Sébastien Duperron

► To cite this version:

Kamil M. Szafranski, Bérénice Piquet, Bruce Shillito, François Lallier, Sébastien Duperron. Relative abundances of methane- and sulfur-oxidizing symbionts in gills of the deep-sea hydrothermal vent mussel *Bathymodiolus azoricus* under pressure. *Deep Sea Research Part I: Oceanographic Research Papers*, 2015, 101, pp.7-13. 10.1016/j.dsr.2015.03.003 . hal-01133684

HAL Id: hal-01133684

<https://hal.sorbonne-universite.fr/hal-01133684>

Submitted on 20 Mar 2015

HAL is a multi-disciplinary open access archive for the deposit and dissemination of scientific research documents, whether they are published or not. The documents may come from teaching and research institutions in France or abroad, or from public or private research centers.

L'archive ouverte pluridisciplinaire **HAL**, est destinée au dépôt et à la diffusion de documents scientifiques de niveau recherche, publiés ou non, émanant des établissements d'enseignement et de recherche français ou étrangers, des laboratoires publics ou privés.

1 **Relative abundances of methane- and sulfur-oxidizing symbionts in gills of the deep-sea**
2 **hydrothermal vent mussel *Bathymodiolus azoricus* under pressure.**

3

4 Kamil M. Szafranski^{1,2*}, Bérénice Piquet^{1,2}, Bruce Shillito^{1,2}, François H. Lallier^{3,4} and Sébastien
5 Duperron^{1,2,5}

6 1 Sorbonne Universités, UPMC Univ Paris 06, UMR 7208, Adaptation aux Milieux Extrêmes –
7 Paris, France

8 2 UMR MNHN UPMC CNRS IRD UCBN 7208 Biologie des Organismes Aquatiques et
9 Ecosystèmes, 75005 Paris, France

10 3 Sorbonne Universités, UPMC Univ Paris 06, UMR 7144, Equipe ABICE, Station Biologique de
11 Roscoff, 29680 Roscoff, France

12 4 CNRS, UMR 7144, Adaptation et Diversité en Milieu Marin, Station Biologique de Roscoff,
13 29680 Roscoff, France

14 5 Institut Universitaire de France, Paris, France

15 * Corresponding author: km.szafranski@gmail.com

16 Present address: Université Paris-Sud,

17 Unité d'Ecologie, Systématique et Evolution, CNRS UMR 8079

18 91405 Orsay cedex, France

19 Phone: +33 (0)1 69 15 61 15

20

21 **Running title:** Symbiont abundances in *Bathymodiolus azoricus* under pressure

22 **Keywords:** 3D FISH; hydrothermal vents; pressurized recovery; symbiosis; symbiont
23 quantification; mussels

24 **Abstract**

25 The deep-sea mussel *Bathymodiolus azoricus* dominates hydrothermal vent fauna in the the Azores
26 region. The gills of this species house methane- and sulfur-oxidizing bacteria that fulfill most of the
27 mussel's nutritional requirements. Previous studies suggested that the ratio between methane- and
28 sulfur-oxidizers could vary in response to the availability of electron donors in their environment,
29 and this flexibility is considered a key factor in explaining the ecological success of the species.
30 However, previous studies were based on non-isobaric recovery of specimens, with experiments at
31 atmospheric pressure which may have induced artifacts. This study investigates the effect of
32 pressure-related stress during recovery and experimentation on the relative abundances of bacterial
33 symbionts. Mussel specimens were recovered for the first time using the pressure-maintaining
34 device PERISCOP. Specimens were subsequently transferred into pressurized vessels and exposed
35 to various chemical conditions. Using optimized fluorescence *in situ* hybridization-based
36 approaches, relative abundance of symbionts were measured. Our results show that the recovery
37 method (isobaric versus non-isobaric) does not influence the abundances of bacterial symbionts.
38 Significant differences occur among specimens sampled from two contrasting sites. Exposure of
39 mussels from the deeper site to sulfide and bicarbonate, and to bicarbonate alone, both resulted in a
40 rapid and significant increase in the relative abundance of sulfur-oxidizers. Results reported herein
41 are congruent with those from previous reports investigating mussels originating from shallow sites
42 and kept at ambient pressure. Isobaric recovery and maintenance allowed us to perform *in vivo*
43 experiments in specimens from a deeper site that could not be maintained alive at ambient pressure,
44 and will greatly improve the chances of identifying the molecular mechanisms underlying the
45 dialogue between bathymodioline hosts and symbionts.

46 **Introduction**

47 Bathymodiolinae mussels (family Mytilidae) are part of the remarkable fauna colonizing
48 ecosystems such as hydrothermal vents and cold seeps in the deep-sea (Desbruyères et al., 2000;
49 Duperron, 2010; Duperron et al., 2009; von Cosel et al., 1999, 2001). These mussels rely upon
50 sulfur- or methane-oxidizing (SOX and MOX) bacteria occurring in their gill epithelial cells for all
51 or part of their nutrition (Cavanaugh et al., 1981; Felbeck, 1981). The symbionts of mussels exploit
52 compounds present in vent or seep fluids for their metabolism (Van Dover, 2000; Van Dover et al.,
53 2002). Although sulfide is toxic to animals, symbiotic sulfur-oxidizers use hydrogen sulfide from
54 the fluids as the source of energy for their metabolism and to fix inorganic carbon (Cavanaugh et
55 al., 1988). Methane-oxidizing bacteria use methane both as a carbon and an energy source
56 (Cavanaugh et al., 1992; Childress et al., 1986). Organic carbon compounds are subsequently
57 transferred to their animal host and ultimately contribute to ecosystem productivity in habitats
58 where only a small fraction of the photosynthetic primary production from upper layers of the
59 oceans is brought in by sedimentation or advective transport (Cavanaugh, 1983; Corliss et al., 1979;
60 Karl et al., 1980).

61 *Bathymodiolus azoricus* and its sister species *B. puteoserpentis* dominate several vent sites on the
62 Mid-Atlantic Ridge (MAR). They possess both sulfur- and methane-oxidizing symbionts in their
63 gill bacteriocytes, as demonstrated through ultrastructural studies, 16S rRNA-encoding gene
64 sequence analyses, and enzyme assays (Cavanaugh et al., 1992; Distel et al., 1995; Duperron et al.,
65 2006; Fiala-Medioni et al., 2002; Fisher et al., 1993). Dual symbiosis is thought to increase the
66 environmental tolerance of hosts because the distinct metabolism of the sulfur- and methane-
67 oxidizing symbionts may help the holobiont adapt to varying availability of reduced sulfur and
68 methane (Distel et al., 1995; Fiala-Medioni et al., 2002). Several studies point to a high flexibility
69 of the symbiont populations (Kádár et al., 2005; Riou et al., 2008). Bacteria indeed disappear from
70 *B. azoricus* gill bacteriocytes when subjected to starvation in sulfide- and methane-free sea-water,
71 but can be recovered when mussels return to sulfide-enriched aquaria (Kádár et al., 2005). The
72 relative volume occupied by each symbiont type in bacteriocytes of *B. azoricus* varies within vent
73 sites, and between sites displaying different chemical signatures (Halary et al., 2008). Experiments
74 using mussels maintained in controlled conditions at atmospheric pressure with one, both or none of
75 the electron donors necessary for endosymbiont metabolism confirm that symbiont relative
76 abundances can change rapidly in response to changes in the availability of their respective
77 substrates (Halary et al., 2008; Riou et al., 2010, 2008).

78 However, the previously mentioned results suffer numerous potential biases. First, specimen
79 recovery from the MAR vent sites, which are located at depths between 800 m (Menez Gwen) and

80 3500 m (Logatchev), involved rapid (usually a few hours) and large de-pressurization of specimens
81 (8 to 35 MPa). This results in high levels of stress, ultimately resulting in the death of specimens
82 from the deepest sites (Halary et al., 2008). Second, specimens used in *in vivo* experiments are
83 usually from shallower vent sites (Menez Gwen) and maintained in the laboratory at atmospheric
84 pressure, *i. e.* ~80-fold lower than *in situ* conditions (Kádár et al., 2005; Riou et al., 2008). Results
85 from these studies are thus potentially affected by artifacts associated with depressurization, and it
86 remains to be confirmed whether observed symbiont dynamics were the consequence of these
87 stresses or true biological responses. Another issue is with the quantification of symbionts itself.
88 Several studies are based on a 3D fluorescence *in situ* hybridization (FISH) approach, which
89 measures the fraction of the total volume occupied by each type of symbiont within bacteriocytes
90 (Halary et al., 2008; Riou et al, 2008; Duperron et al, 2011). Although reliable, this approach is time
91 consuming because it involves the acquisition of 3D images of gill sections, manual cropping of
92 individual bacteriocytes, and computing volumes using a dedicated ImageJ plugin (Halary et al.,
93 2008). This has limited the number of specimens that could be analyzed, reducing the statistical
94 power of comparisons (Prosser, 2010).

95 Several pressurized vessels for live maintenance and pressurized recovery that prevent or reduce
96 pressure-related stress have become available in recent years (Boutet et al., 2009). The first aim of
97 the present study is to investigate relative symbiont abundances in *B. azoricus* mussels recovered
98 from the Menez Gwen (800 m depth) and Rainbow (2300 m depth) vent sites using the pressure-
99 maintaining PERISCOP sampling cell (Shillito et al., 2008). The second aim is to investigate these
100 abundances in Rainbow specimens exposed to substrates used by the sulfide-oxidizing bacteria at
101 their native pressure in the IPOCAMP vessel (Shillito et al., 2014). The percentage of total bacterial
102 volume corresponding to methane- plus sulfur-oxidizing symbionts is measured by means of FISH
103 and image analysis. In order to optimize the method, we compare results from three FISH-based
104 approaches, and images acquired from the anterior and posterior regions of the gills. We then
105 compare isobaric *vs.* non-isobaric recovery, Menez Gwen and Rainbow specimens, and the effect of
106 treatments applied to live specimens from Rainbow. Results are discussed in relation to
107 improvements of the methods used to investigate symbiont dynamics in animal tissue in light of
108 previous reports, based on specimens from non-isobaric recoveries and exposed to various
109 experimental conditions at atmospheric pressure.

110 **Material and methods**

111 *Sampling sites*

112 *Bathymodiolus azoricus* mussels (Bivalvia, Mytilidae) (von Cosel et al., 2001) were collected from
113 two hydrothermal vent sites during the 2013 BioBaz cruise to the Mid-Atlantic Ridge aboard RV

114 *Pourquoi Pas?* using the ROV *Victor 6000*. Specimens were sampled from the vicinity of active
115 smokers at Menez Gwen (MG2 marker, 37°50.669' N 31°31.156' W, 830 m depth) and Rainbow
116 (France5 marker, 36°13.766' N 33°54.117' W, 2270 m depth) (Figure 1). Active vents were
117 colonized by fauna typical for MAR vents, including one bivalve (*Bathymodiolus azoricus*) and
118 three shrimp species (*Rimicaris exoculata*, *Mirocaris fortunata* and *Chorocaris chacei*)
119 (Desbruyères et al., 2001).

120 *Isobaric and non-isobaric recovery*

121 At each sampling site, specimens were recovered in clean watertight BioBoxes, which were brought
122 to the surface by the ROV or the shuttle within a few hours (non-isobaric sampling). Others were
123 placed inside a 'CROCO' sampling cell that was fit into the pressure-keeping vessel PERISCOP
124 (isobaric recovery, Shillito et al., 2008). PERISCOP was then closed and the shuttle to which it was
125 attached was released within a few minutes, and surfaced within 45 minutes. Pressure was
126 monitored during surfacing with autonomous pressure sensor (SP2T4000, NKE Instruments,
127 France). Once onboard, PERISCOP was opened and mussels were recovered and either dissected
128 and fixed, or transferred to the IPOCAMP pressure vessel within 10 minutes.

129 *Exposure to bicarbonate and sulfide in pressurized vessels*

130 Six mussels from Rainbow, recovered using the PERISCOP, were taken out and used in incubation
131 experiments (shell length: 44.4-100.5 mm). Due to the limited volume of the IPOCAMP chamber
132 and the size of specimens, only two specimens were transferred in each of three 1 liter Nalgene™
133 bottles filled with 11.8 µM NaHCO₃ and 36.4 µM Na₂S; with 11.8 µM NaHCO₃; or with filtered
134 sea-water alone (control). These concentrations were within the range of values recorded in mussel
135 aggregates on the site, and similar to values used in previous studies (Halary et al., 2008; Riou et al,
136 2008). Bottles were tightly closed and re-pressurized in IPOCAMP aquariums within 5 minutes.
137 Mussels were incubated at 23MPa and 8°C for 5 h, then dissected immediately and fixed.

138 *Sample fixation onboard*

139 Anterior and posterior parts of mussel gill tissue were dissected at 4°C and fixed for fluorescence *in*
140 *situ* hybridization (FISH). Gill fragments were transferred to 4% formaldehyde in twice-filtered sea-
141 water (TFSW) (4°C, 2–4 h), rinsed, and dehydrated in increasing ethanol (50, 70 80, and 96%, 15
142 min each). The density of gill filaments per millimeter was measured under a dissecting
143 microscope.

144 *Fluorescence in situ hybridization (FISH)*

145 Fragments of gills were embedded in polyethylene glycol distearate (PEG):1-hexadecanol (9:1), cut
146 into 8 µm-thick sections and deposited on SuperFrost Plus slides (VWR International, USA). Wax

147 was removed and tissue rehydrated in decreasing ethanol series (96% to 70%). Sections were
148 hybridized using 40% formamide for 1–3 h at 46°C as previously described (Duperron et al., 2008),
149 rinsed, and mounted in DAPI-containing “Slow Fade” (Life Technologies) under a coverslip. Three
150 16S rRNA-specific probes were applied simultaneously on every section. FISH probes used are
151 summarized in Table 1.

152 *Image acquisition and analysis*

153 Slides were observed under a BX61 epifluorescence (Olympus, Japan) or a SP5 confocal (Leica,
154 Germany) microscope, and images were acquired at 400x magnification using ImagePro 6.0
155 (Olympus, Japan). On each section, a 2D image was first acquired by overlaying signals from the
156 three probe-associated fluorochromes (2D acquisition). Second, an image stack was built by
157 acquiring images every 0.3 μm over the thickness of the section (3D acquisition). Images were
158 analyzed using ImageJ (Abramoff et al., 2004) and the total volume occupied by bacteria and
159 respective proportions of the sulfur- and methane-oxidizing symbionts were computed for 2D and
160 3D images using the SymbiontJ plug-in as previously described, but applying the procedure to the
161 whole field of view without isolating individual bacteriocytes (Halary et al., 2008). SymbiontJ
162 applies filters and thresholds to the different color channels and computes the number of voxels
163 corresponding to each symbiont type. Finally, ten bacteriocytes were manually cropped from each
164 3D acquisition, analyzed using SymbiontJ, and the mean percentage of volume occupied by each
165 bacterial type was computed (bacteriocyte acquisition).

166 *Statistical analyses*

167 The percentage of bacterial volume occupied by methane-oxidizing bacteria was used for all
168 analyses, after an Arcsine transformation (Halary et al., 2008). Values were then used for
169 transformation-based redundancy analyses (tb-RDA). Sampling site (Menez Gwen versus
170 Rainbow), recovery mode (isobaric versus non-isobaric), acquisition method (2D, 3D or
171 bacteriocyte), gill region (anterior versus posterior), and specimen were used as factors into the
172 constrained redundancy analysis (RDA), in order to estimate their contribution to the global
173 variance. Significance was assessed using permutation tests ($n=9999$) using a full model, with
174 separate test for each term (constraining variable). Shapiro-Wilk tests revealed non-normal
175 distribution of the data, and non-parametric tests were thus applied for inter-groups comparisons.
176 The Mann-Whitney-Wilcoxon (MWW, for 2 class factors) and Kruskal-Wallis (KW, for 3 or more
177 class factors) tests were used to compare percentages of methanotrophs. All statistical analyses were
178 performed using R (R Development Core Team, 2013); 'vegan' package was used for the
179 constrained redundancy analysis.

180 **Results**

181 In order to optimize the 3D FISH method (Halary et al., 2008), three types of images were acquired
182 and compared. For each mussel specimen, 10 acquisitions in 2D and 10 in 3D were obtained. From
183 each of the later 3D acquisitions, 10 randomly chosen bacteriocytes were analyzed, resulting in 100
184 bacteriocytes per specimen. These acquisitions were obtained from at least 5 different sections, each
185 containing 10-20 filaments. Results are summarized in Table 2, and a micrograph showing gill
186 tissue with bacteriocytes containing the two symbionts is presented on Figure 2. The analyses of
187 2D, 3D, and bacteriocytes did not yield significantly different results (KW test on all measurements
188 including anterior and posterior gill regions, p-value = 0.09).

189 The filament density per mm gill length along the anterior-posterior axis decreased significantly
190 with increasing shell length ($R^2=65\%$, Pearson's correlation test: p-value < 0.001, Figure 3). Gills
191 form and grow from the posterior end. Percentages of methanotrophs (MOX) in the anterior and
192 posterior regions of gill from 3 specimens per treatment (12 specimens) were computed using 2D
193 and 3D methods, yielding in total 480 measurements (Table 2, Table S1). The percentage of volume
194 occupied by methanotrophs was not significantly different between anterior and posterior regions of
195 the gills (MWW test, p-value = 0.64). Subsequent analyses were thus made only on the anterior part
196 of gills, for which more specimens were available.

197 When recovered in BioBoxes, mussels from Menez Gwen and Rainbow experienced pressure loss
198 of around 8.3 and 23 MPa, respectively. The use of PERISCOP prevented that, and mussels arrived
199 onboard at pressures close to those of the deep waters (Table 2). Percentages of volume occupied by
200 methanotrophs were $46.5\% \pm 5.8$ and $56.3\% \pm 6.4$ in Menez Gwen and Rainbow mussels recovered
201 in BioBoxes, and $44.3\% \pm 5.7$ and $56.3\% \pm 8.3$ in mussels recovered using PERISCOP (Figure 4,
202 Table 2). A MWW test based on 1140 values from the anterior and posterior regions of the gills
203 indicated no significant difference between the two types of recovery (p-value = 0.12).

204 Mussels from Menez Gwen and Rainbow sites displayed significantly different percentages of
205 methanotrophs in their gills (MWW test, $W = 36185.5$, p-value < $2.2e-16$). A unilateral test
206 confirmed that methanotrophs occupied a higher fraction of the overall volume in bacteriocytes of
207 *B. azoricus* from the deeper Rainbow site (Figure 4, Table 2, Table S1).

208 The influence of each aforementioned factor was estimated by constrained redundancy analysis
209 (RDA) and ANOVA permutation tests. Overall, our model could explain 56% of the total variance.
210 Sampling site was the most influential factor (41%; df = 1; F = 1026.1), followed by inter-
211 individual differences, which accounted for more than 14% (df = 27; F = 13.3) of the total variance.
212 Other factors explained much lower fractions of the variance: recovery mode (0.3%; df = 1; F =
213 7.7), acquisition method (0.3%; df = 2; F = 3.8) and gill region (0.04%; df = 1; F = 0.1) (Table S2).

214 Each experimental condition could be applied to 2 specimens only from Rainbow because of the

215 limited volume of bottles and the limited number of bottles that could be incubated at once in
216 pressurized vessels. Nevertheless, 2 different treatments ($\text{NaHCO}_3 + \text{Na}_2\text{S}$ or NaHCO_3 alone) and 2
217 control experiments (10 mussels fixed immediately after recovery using PERISCOP and 2
218 incubated in filtered sea-water in the same conditions as above) were applied, and 320
219 measurements were made using 2D and 3D methodologies (Figure 5, Table S3). There was no
220 significant difference between 2D and 3D FISH acquisition methods in this dataset (MWW test, p-
221 value = 0.54). The different treatments under pressure resulted in significant differences in
222 percentages of methanotrophs (KW test, p-values < 0.011). The percentage of sulfur-oxidizers was
223 twice higher in specimens exposed to sulfide and bicarbonate than in the sea-water treatment, with
224 $90.1\% \pm 17.6$ versus $38.5\% \pm 4.9$ (Figure 5, Table S3). Specimens exposed to bicarbonate alone
225 also displayed a markedly higher percentage of sulfur-oxidizers (SOX) than in the sea-water
226 treatment. SOX in the bicarbonate treatment occupied $76.0\% \pm 23.0$ of the bacterial volume. The
227 percentage of SOX was slightly lower in mussels incubated in filtered seawater than prior to
228 treatments (38.5 ± 4.9 versus $42.5\% \pm 7.6$). Constrained RDA indicated that the overall variance
229 was mainly explained by the 'treatment' factor (68.5%; $df = 3$; $F = 506.7$) and by inter-individual
230 variability (18%; $df = 12$; $F = 32.8$), while 0.4% ($df = 1$; $F = 0.9$) was due to the method of image
231 acquisition (Table S4).

232 **Discussion**

233 *Image based quantification of volumes occupied by symbionts*

234 Three FISH approaches were applied in this study, based on acquisition of 2D (Figure 2A) and 3D
235 images, and of individual bacteriocytes (Figure 2B). They did not yield significantly different
236 results. Although the results are similar, the bacteriocyte-based method used in previous studies
237 (Riou et al., 2010) is by far the most time-consuming, because it involves manually cropping and
238 computing percentages of methanotrophs in at least 10 bacteriocytes from each 3D image. If the
239 aim is to maximize the number of acquisitions, the 2D or 3D approaches are equally suitable and far
240 less time-consuming. In this study we managed to analyze a total of 36 specimens with two to three
241 of these methods (Table 2), while previous studies using 3D-FISH were based 20 or fewer
242 individuals (Duperron et al., 2011, 2007; Halary et al., 2008; Lorion et al., 2012; Riou et al., 2010,
243 2008).

244 *Sampling methodology*

245 The density of gill filaments was negatively related to shell length, *i.e.* the longer the shell was, the
246 less dense gill filaments were (Figure 3). Similar filament densities and size-related trend are
247 reported for the mussel *Mytilus edulis* (Jones et al., 1992). The gill forms and grows from the
248 posterior end in bivalves (Cannuel et al., 2009; Wentrup et al., 2014); this process could result in

249 differences in symbiont relative abundances between the 'young' posterior part and 'old' anterior
250 one, but this was not confirmed by our data. It is likely that the absolute number of symbionts in
251 each filament, which was not computed here, is different in the respective gill regions, in particular
252 in the posterior-most budding zone (Wentrup et al., 2014). Measuring absolute numbers of
253 symbionts would be necessary, but a reliable method still remains to be implemented (Boutet et al.,
254 2011).

255 The two sites analyzed differed in depth (850 m at Menez Gwen and 2300 m at Rainbow) but non-
256 isobaric recovery in BioBoxes involved significant pressure loss and potential physiological stress
257 in both cases. Recovery stress is a major criticism often addressed to deep-sea biologists and
258 physiologists by many colleagues who are dubious about reports from *ex situ* experiments. In the
259 present study, mussels were for the first time recovered under their natural pressure until opening of
260 the PERISCOP vessel on board, and compared with specimens recovered using classical, non-
261 isobaric BioBoxes. Results indicate that, as far as symbiont relative abundances in gills are
262 concerned, the recovery mode did not have any significant influence, not even for the deeper
263 Rainbow site (Figure 4). This major finding validates *a posteriori* previous studies dealing with
264 symbiont relative abundances that did use classical non-isobaric recovery methods involving
265 pressure loss (Duperron et al., 2011, 2006; Halary et al., 2008; Lorion et al., 2012; Riou et al., 2010,
266 2008). However, although non-isobaric sampling is appropriate for studies focusing on symbiont
267 relative abundances, isobaric recovery probably makes a difference when dealing with
268 physiological parameters such as host and symbiont activities and gene expression. FISH signal
269 intensities (but not areas and volumes) were indeed usually higher in specimens recovered using
270 PERISCOP, suggesting that ribosomes to which FISH probes attach were less abundant in the latter
271 (unpublished data).

272 *Site-related differences in symbiont abundances*

273 Besides depth, the Menez Gwen and Rainbow sites differ by several characteristics, including the
274 chemical composition of end-member fluids. Fluids at Menez Gwen indeed display slightly lower
275 concentrations of methane compared to Rainbow (Charlou et al., 2002). Sulfide concentrations are
276 similar, but sulfide interacts with the high concentrations of iron at Rainbow, and is thus not readily
277 available to organisms (Desbruyères et al., 2000; Le Bris and Duperron, 2010). Geochemical
278 modeling applied to the mixing zone where mussels actually live indicate that more energy can be
279 gained from sulfide at Menez Gwen compared to methane, while the opposite situation is
280 encountered at Rainbow (Le Bris and Duperron, 2010). The result at Rainbow is however less clear-
281 cut when including hydrogen, an alternative energy source for sulfur-oxidizing symbionts (Petersen
282 et al., 2011). The ratio between sulfide and methane has been shown to influence the relative

283 abundance of sulfur- versus methane-oxidizers in mussel gills, and methanotrophs are more
284 abundant than thiotrophs at Rainbow (Duperron et al., 2006). Previous estimations of symbiont
285 relative abundances indicated that sulfur-oxidizers represented $53.1\% \pm 10.3$ of the total volume of
286 symbionts at Menez Gwen, compared to 39.4% at Rainbow (Halary et al., 2008; Le Bris and
287 Duperron, 2010). Our results from PERISCOP-recovered specimens were remarkably close (52.6%
288 ± 4.9 and $43.7\% \pm 6.4$ respectively; Table 2). This is in line with the hypothesis that symbiont
289 relative abundances depend on the availability of their respective substrates (Fiala-Medioni et al.,
290 2002; Riou et al., 2008; Trask and Van Dover, 1999). Furthermore, the unexpected similarity
291 between measurements made on specimens sampled in 2006 and 2013 suggests a certain level of
292 long term stability in site-related differences, although short-term fluctuations certainly have
293 occurred (Duperron et al., 2006; Halary et al., 2008).

294 *Symbiont response to bicarbonate and sulfide pulses under pressure*

295 Starvation experiments and exposure to increased concentrations of different chemosynthesis
296 substrates have already been performed by several groups (Halary et al., 2008; Kádár et al., 2005;
297 Riou et al., 2008), but most often on *B. azoricus* from the shallower Menez Gwen site and at
298 ambient pressure. Here, we tested the effect of sulfide and bicarbonate exposure on pressurized *B.*
299 *azoricus* from the deeper Rainbow site (2300 m depth). Mussels from this site are not easily
300 maintained in the lab at ambient pressure (authors' personal observation). PERISCOP-recovered
301 mussels were transferred to pressure vessels and maintained at 8°C and 23 MPa. A 5h incubation
302 period with bicarbonate and sulfide resulted in doubling of the relative abundance of thiotrophs in
303 the gills (Figure 5). Exposure to bicarbonate alone also significantly increased the relative
304 abundance of thiotrophs (Figure 5). These rapid changes confirm that observations reported in
305 Halary et al. 2008 and other works on mussels from Menez Gwen were not artifacts, and not linked
306 to recovery stress or experimentation at atmospheric pressure. The increase in thiotroph relative
307 volume observed in the present study is even more spectacular (65.0% in Halary et al., 2008). In
308 another study, mussels subjected to a one-month starvation followed by 4 days of constant sulfide
309 supply showed a 96% bacterial volume occupation by thiotrophs (Riou et al., 2008). Here, we show
310 that non-starved *B. azoricus* can shift to an almost thiotrophic symbiosis within 5 hours of exposure
311 to sulfide and bicarbonate (Figure 5). Unfortunately, only two specimens could be subjected to each
312 treatment because of space limitations in IPOCAMP. So although the trend is clear, data from more
313 specimens is needed to reliably estimate the true amplitude of this effect. Thiotrophic symbionts fix
314 inorganic carbon using ribulose-1,5-bisphosphate Carboxylase Oxygenase (RubisCO) in the Calvin
315 cycle (Cavanaugh et al., 1988). This process requires energy from the oxidation of reduced sulfur
316 compounds (Cavanaugh et al., 1988). The less spectacular increase in relative abundance of

317 thiotrophs when only bicarbonate was available also suggests that another source of energy may
318 have been used for chemosynthesis. Over a short period, bacteria might have used sulfur stored in
319 compounds such as taurine or thiotaurine (Pruski and Fiala-Médioni, 2003). Alternatively,
320 hydrogen, not measured in our study, has been demonstrated to be an alternative energy source for
321 hydrothermal vent symbioses (Amend and Shock, 2001; Petersen et al., 2011). Although the
322 increase in thiotrophs relative abundance could result directly from an actual increase in their
323 number, it could alternatively result from a decrease in methanotrophs, whose substrate was absent
324 and which may have been digested by host bacteriocytes before thiotrophs. Methanotrophs are
325 indeed located more basally within bacteriocytes, closer to phagolysosome-like bodies (Distel et al.,
326 1995; Duperron et al., 2005). It is not known which mechanisms on the host and symbionts sides
327 control the dynamics of bacterial populations within bacteriocytes. Mussel symbionts have been
328 shown to divide and to be digested within bacteriocytes, but additional mechanisms may explain
329 their variations, including symbiont uptake from the environment by adults, as suggested in *B.*
330 *brevior*, and symbiont release as documented in corals (Dubilier et al., 1998; Lesser, 2011; Thurber
331 et al., 2009). Whatever the underlying mechanisms, the symbiont population as a whole seems to be
332 rapidly and significantly affected by changes in the availability of energy and carbon sources,
333 although results from more specimens are necessary.

334 **Conclusions**

335 In this study, a FISH-based method was used to quantify relative abundances of endosymbionts in
336 gills of *Bathymodiolus azoricus*. Abundances in the anterior and posterior regions of the gill were
337 similar. Mussels sampled in isobaric and non-isobaric recovery devices displayed similar relative
338 volumes of the two types of symbionts indicating that non-isobaric recovery does not induce a
339 major bias in measured volume occupation. However, the physiological status of mussels and their
340 endosymbionts is probably not the same and isobaric recovery is certainly to be recommended for
341 physiological or expression studies of specimens from the deepest sites. Symbiont relative volumes
342 were different between the Menez Gwen and Rainbow sites, and similar to those previously
343 measured on specimens sampled 7 years ago. On the other hand, symbiont populations displayed
344 high flexibility in exposure experiments performed in pressurized aquaria. As postulated previously,
345 this flexibility is certainly an advantage because physico-chemical micro-environments at
346 hydrothermal vents are highly variable in time and space (Chevaldonné et al., 1991; Johnson et al.,
347 1994, 1986; Le Bris et al., 2005), and maybe the key for the domination of *Bathymodiolus azoricus*
348 at various hydrothermal vent sites of the Mid-Atlantic Ridge (Desbruyères et al., 2001, 2000; Von
349 Cosel et al., 1999). More experiments involving methane, hydrogen, toxic compounds, but also
350 thermal stress and symbiont release experiments will be necessary to further explore this flexibility.

351 The next step will then be to unravel the mechanisms that control this flexibility by exploring cell
352 division patterns, genes and protein expressions of host and symbionts in various conditions.

353 **Acknowledgments**

354 We thank the captain and crew of RV “Pourquoi Pas?” and ROV “Victor 6000” for their invaluable
355 help onboard. We are grateful to M. Zbinden, J-Y. Collet, J-B. Collet and A. Tanguy for their help
356 with samples and aquaria onboard, and V. Le Layec for his help in the lab. This research was
357 supported by CNRS, UPMC, UCBN and ITN Symbiomics. K. Szafranski was funded through a
358 Ph.D. grant from the Marie Curie Actions Initial Training Network (ITN) SYMBIOMICS (contract
359 number 264774). The authors would like to thank the reviewers and editors for their comments that
360 helped to improve the manuscript.

361 **Table legends**

362 Table 1: Probes, target groups, and labels used in FISH experiments.

363 Table 2: Sites, number of individuals, and percentages of methane- (MOX), and sulfur-oxidizers
364 (SOX), standard deviation (SD) measured using the 2D, 3D, and bacteriocyte-based FISH methods
365 in the anterior region of the gill. Maintained pressure during recovery has been calculated as follow:
366 $P_{\min}/P_{\max} \times 100\%$, where P_{\max} is the pressure at sampling site, P_{\min} – the minimal pressure during
367 recovery.

368 Table S1: Sites, number of individuals, and percentages of methane- (MOX), and sulfur-oxidizers
369 (SOX), standard deviation (SD) measured using the 2D and 3D -based FISH methods in the
370 posterior region of the gill.

371 Table S2: Redundancy analysis estimating the contribution of factors site (SITE), recovery method
372 (REC), FISH method (METH), localization in the gill (GILL), and inter-individual variability
373 (IND) to the variability observed in percentages of methane-oxidizers in gills among Menez Gwen
374 and Rainbow specimens.

375 Table S3: Percentages of methane- (MOX), and sulfur-oxidizers (SOX) and standard deviation (SD)
376 measured using the 2D- and 3D -based FISH methods in the anterior region of the gill of Rainbow
377 specimens upon recovery using PERISCOP (T0) and those exposed to 5-hours experimental
378 treatments in pressurized vessels at 23 MPa.

379 Table S4: Redundancy analysis estimating the contribution of factors treatment (TREAT), FISH
380 method (METH), and inter-individual variability (IND) in the variance observed in percentages of
381 methane-oxidizers in gills among Rainbow specimens exposed to chemical treatments in
382 pressurized vessels.

383 **Figure legends**

384 Figure 1: Localization of sampling sites on the Mid-Atlantic Ridge. MG – Menez Gwen site (830 m
385 depth); Rb – Rainbow site (2270 m depth).

386 Figure 2: Overview (A) and detail (B) of transverse sections through *B. azoricus* gill filaments
387 observed at 400× magnification. Filaments were cut parallel to the plane defined by the animals
388 anterior-posterior and left-right axes, and perpendicular to its dorso-ventral axis. Nuclei from host
389 tissue are labeled with DAPI (blue). FISH-labeled bacterial symbionts appear in pink (sulfur-
390 oxidizers) and green (methanotrophs).

391 Figure 3: Density of gill filaments versus antero-posterior length of the shell. Fitted line is a linear
392 regression ($R^2=65\%$, Pearson's correlation test: p-value < 0.001).

393 Figure 4: Mean percentage and standard deviation of total bacterial volume occupied by methane-
394 oxidizers in gill tissue of *B. azoricus* specimens from Menez Gwen and Rainbow recovered in
395 BioBoxes (non-isobaric) and PERISCOP vessels (isobaric). Shades of grey correspond to the three
396 FISH methods as indicated (see text for details).

397 Figure 5: Mean percentage and standard deviation of total bacterial volume occupied by sulfur-
398 oxidizers in gill tissue of *B. azoricus* specimens from Rainbow upon recovery using PERISCOP
399 (T0) and exposed to experimental treatments in pressurized vessels ($\text{NaHCO}_3 + \text{Na}_2\text{S}$, NaHCO_3 ,
400 filtered sea-water). Shades of grey correspond to the two FISH methods as indicated (see text for
401 details).

402 **References**

- 403 Abramoff, M., Magelhaes, P., Ram, S., 2004. Image Processing with ImageJ. *Biophotonics Int.* 11,
404 36–42.
- 405 Amann, R.L., Binder, B.J., Olson, R.J., Chisholm, S.W., Devereux, R., Stahl, D.A., 1990.
406 Combination of 16S rRNA-targeted oligonucleotide probes with flow cytometry for
407 analyzing mixed microbial populations. *Appl. Environ. Microbiol.* 56, 1919–1925.
- 408 Amend, J.P., Shock, E.L., 2001. Energetics of overall metabolic reactions of thermophilic and
409 hyperthermophilic Archaea and Bacteria. *FEMS Microbiol. Rev.* 25, 175–243.
- 410 Boutet, I., Jollivet, D., Shillito, B., Moraga, D., Tanguy, A., 2009. Molecular identification of
411 differentially regulated genes in the hydrothermal-vent species *Bathymodiolus thermophilus*
412 and *Paralvinella pandorae* in response to temperature. *BMC Genomics* 10, 222.
- 413 Boutet, I., Ripp, R., Lecompte, O., Dossat, C., Corre, E., Tanguy, A., Lallier, F.H., 2011.
414 Conjugating effects of symbionts and environmental factors on gene expression in deep-sea
415 hydrothermal vent mussels. *BMC Genomics* 12, 530.
- 416 Cannuel, R., Beninger, P.G., McCombie, H., Boudry, P., 2009. Gill development and its functional
417 and evolutionary implications in the blue mussel *Mytilus edulis* (Bivalvia: Mytilidae). *Biol.*
418 *Bull.* 217, 173–188.
- 419 Cavanaugh, C.M., 1983. Symbiotic chemoautotrophic bacteria in marine invertebrates from
420 sulphide-rich habitats. *Nature* 302, 58–61.
- 421 Cavanaugh, C.M., Abbott, M.S., Veenhuis, M., 1988. Immunochemical localization of ribulose-1,5-

- 422 bisphosphate carboxylase in the symbiont-containing gills of *Solemya velum* (Bivalvia:
423 Mollusca). Proc. Natl. Acad. Sci. U. S. A. 85, 7786–7789.
- 424 Cavanaugh, C.M., Gardiner, S.L., Jones, M.L., Jannasch, H.W., Waterbury, J.B., 1981. prokaryotic
425 cells in the hydrothermal vent tube worm *Riftia pachyptila* Jones: possible
426 chemoautotrophic symbionts. Science 213, 340–342.
- 427 Cavanaugh, C.M., Wirsén, C.O., Jannasch, H.W., 1992. Evidence for methylotrophic symbionts in a
428 hydrothermal vent mussel (bivalvia: mytilidae) from the mid-atlantic ridge. Appl. Environ.
429 Microbiol. 58, 3799–3803.
- 430 Charlou, J.L., Donval, J.P., Fouquet, Y., Jean-Baptiste, P., Holm, N., 2002. Geochemistry of high H₂
431 and CH₄ vent fluids issuing from ultramafic rocks at the Rainbow hydrothermal field
432 (36°14'N, MAR). Chem. Geol. 191, 345–359.
- 433 Chevaldonné, P., Desbruyères, D., Haïtre, M.L., 1991. Time-series of temperature from three deep-
434 sea hydrothermal vent sites. Deep Sea Res. Part Oceanogr. Res. Pap. 38, 1417–1430.
- 435 Childress, J.J., Fisher, C.R., Brooks, J.M., Kennicutt, M.C., Bidigare, R., Anderson, A.E., 1986. A
436 methanotrophic marine molluscan (bivalvia, mytilidae) symbiosis: mussels fueled by gas.
437 Science 233, 1306–1308.
- 438 Corliss, J.B., Dymond, J., Gordon, L.I., Edmond, J.M., Herzen, R.P. von, Ballard, R.D., Green, K.,
439 Williams, D., Bainbridge, A., Crane, K., Andel, T.H. van, 1979. Submarine Thermal
440 Springs on the Galápagos Rift. Science 203, 1073–1083.
- 441 Desbruyères, D., Almeida, A., Biscoito, M., Comtet, T., Khripounoff, A., Bris, N.L., Sarradin, P.M.,
442 Segonzac, M., 2000. A review of the distribution of hydrothermal vent communities along
443 the northern Mid-Atlantic Ridge: dispersal vs. environmental controls. Hydrobiologia 440,
444 201–216.
- 445 Desbruyères, D., Biscoito, M., Caprais, J.-C., Colaço, A., Comtet, T., Crassous, P., Fouquet, Y.,
446 Khripounoff, A., Le Bris, N., Olu, K., Riso, R., Sarradin, P.-M., Segonzac, M.,
447 Vangriesheim, A., 2001. Variations in deep-sea hydrothermal vent communities on the Mid-
448 Atlantic Ridge near the Azores plateau. Deep-Sea Res. I 48, 1325–1346.
- 449 Distel, D.L., Lee, H.K., Cavanaugh, C.M., 1995. Intracellular coexistence of methano- and
450 thioautotrophic bacteria in a hydrothermal vent mussel. Proc. Natl. Acad. Sci. U. S. A. 92,
451 9598–9602.
- 452 Dubilier, N., Windoffer, R., Giere, O., 1998. Ultrastructure and stable carbon isotope composition of
453 the hydrothermal vent mussels *Bathymodiolus brevior* and *B. sp. affinis brevior* from the
454 North Fiji Basin, western Pacific. Mar. Ecol. Prog. Ser. 165, 187–193.
- 455 Duperron, S., 2010. The diversity of deep-sea mussels and their bacterial symbioses, in: Kiel, S.
456 (Ed.), The Vent and Seep Biota, Topics in Geobiology. Springer Netherlands, pp. 137–167.
- 457 Duperron, S., Bergin, C., Zielinski, F., Blazejak, A., Pernthaler, A., McKiness, Z.P., DeChaine, E.,
458 Cavanaugh, C.M., Dubilier, N., 2006. A dual symbiosis shared by two mussel species,
459 *Bathymodiolus azoricus* and *Bathymodiolus puteoserpentis* (Bivalvia: Mytilidae), from
460 hydrothermal vents along the northern Mid-Atlantic Ridge. Environ. Microbiol. 8, 1441–
461 1447.
- 462 Duperron, S., Guezi, H., Gaudron, S.M., Pop Ristova, P., Wenzhöfer, F., Boetius, A., 2011. Relative
463 abundances of methane- and sulphur-oxidising symbionts in the gills of a cold seep mussel
464 and link to their potential energy sources. Geobiology 9, 481–491.
- 465 Duperron, S., Laurent, M.C.Z., Gaill, F., Gros, O., 2008. Sulphur-oxidizing extracellular bacteria in
466 the gills of Mytilidae associated with wood falls. FEMS Microbiol. Ecol. 63, 338–349.
- 467 Duperron, S., Lorion, J., Samadi, S., Gros, O., Gaill, F., 2009. Symbioses between deep-sea mussels
468 (Mytilidae: Bathymodiolinae) and chemosynthetic bacteria: diversity, function and
469 evolution. C. R. Biol. 332, 298–310.
- 470 Duperron, S., Nadalig, T., Caprais, J.C., Sibuet, M., Fiala-Medioni, A., Amann, R., Dubilier, N.,
471 2005. Dual symbiosis in a *Bathymodiolus* sp. mussel from a methane seep on the Gabon
472 continental margin (southeast Atlantic): 16S rRNA phylogeny and distribution of the
473 symbionts in gills. Appl. Environ. Microbiol. 71, 1694–1700.

- 474 Duperron, S., Sibuet, M., MacGregor, B.J., Kuypers, M.M.M., Fisher, C.R., Dubilier, N., 2007.
475 Diversity, relative abundance and metabolic potential of bacterial endosymbionts in three
476 *Bathymodiolus* mussel species from cold seeps in the Gulf of Mexico. *Environ. Microbiol.*
477 9, 1423–1438.
- 478 Felbeck, H., 1981. Chemoautotrophic potential of the hydrothermal vent tube worm, *Riftia*
479 *pachyptila* Jones (Vestimentifera). *Science* 213, 336–338.
- 480 Fiala-Medioni, A., McKiness, Z.P., Dando, P., Boulegue, J., Mariotti, A., Alayse-Danet, A.M.,
481 Robinson, J.J., Cavanaugh, C.M., 2002. Ultrastructural, biochemical, and immunological
482 characterization of two populations of the mytilid mussel *Bathymodiolus azoricus* from the
483 Mid-Atlantic Ridge: evidence for a dual symbiosis. *Mar. Biol.* 141, 1035–1043.
- 484 Fisher, C.R., Brooks, J.M., Vodenichar, J.S., Zande, J.M., Childress, J.J., Jr., R.A.B., 1993. The co-
485 occurrence of methanotrophic and chemoautotrophic sulfur-oxidizing bacterial symbionts in
486 a deep-sea mussel. *Mar. Ecol.* 14, 277–289.
- 487 Halary, S., Riou, V., Gaill, F., Boudier, T., Duperron, S., 2008. 3D FISH for the quantification of
488 methane- and sulphur-oxidizing endosymbionts in bacteriocytes of the hydrothermal vent
489 mussel *Bathymodiolus azoricus*. *ISME J.* 2, 284–292.
- 490 Johnson, K.S., Beehler, C.L., Sakamoto-Arnold, C.M., Childress, J.J., 1986. In situ measurements
491 of chemical distributions in a deep-sea hydrothermal vent field. *Science* 231, 1139–1141.
- 492 Johnson, K.S., Childress, J.J., Beehler, C.L., Sakamoto, C.M., 1994. Biogeochemistry of
493 hydrothermal vent mussel communities: the deep-sea analogue to the intertidal zone. *Deep*
494 *Sea Res.* I 41, 993–1011.
- 495 Jones, H.D., Richards, O.G., Southern, T.A., 1992. Gill dimensions, water pumping rate and body
496 size in the mussel *Mytilus edulis* L. *J. Exp. Mar. Biol. Ecol.* 155, 213–237.
- 497 Kádár, E., Bettencourt, R., Costa, V., Santos, R.S., Lobo-da-Cunha, A., Dando, P., 2005.
498 Experimentally induced endosymbiont loss and re-acquirement in the hydrothermal vent
499 bivalve *Bathymodiolus azoricus*. *J. Exp. Mar. Biol. Ecol.* 318, 99–110.
- 500 Karl, D.M., Wirsén, C.O., Jannasch, H.W., 1980. Deep-Sea primary production at the galapagos
501 hydrothermal vents. *Science* 207, 1345–1347.
- 502 Le Bris, N., Duperron, S., 2010. Chemosynthetic communities and biogeochemical energy
503 pathways along the Mid-Atlantic Ridge: the case of *Bathymodiolus azoricus*, in: Rona, P.A.,
504 Devey, C.W., Dymont, J., Murton, B.J. (Eds.), *Diversity Of Hydrothermal Systems On Slow*
505 *Spreading Ocean Ridges*. American Geophysical Union, pp. 409–429.
- 506 Le Bris, N., Zbinden, M., Gaill, F., 2005. Processes controlling the physico-chemical micro-
507 environments associated with Pompeii worms. *Deep Sea Res.* I 52, 1071–1083.
- 508 Lesser, M.P., 2011. Coral Bleaching: Causes and Mechanisms, in: Dubinsky, Z., Stambler, N.
509 (Eds.), *Coral reefs: an ecosystem in transition*. Springer Netherlands, pp. 405–419.
- 510 Lorion, J., Halary, S., Nascimento, J. do, Samadi, S., Couloux, A., Duperron, S., 2012. Evolutionary
511 history of *Idas* sp. Med (Bivalvia: Mytilidae), a cold seep mussel bearing multiple
512 symbionts. *Cah. Biol. Mar.* 53, 77–87.
- 513 Petersen, J.M., Zielinski, F.U., Pape, T., Seifert, R., Moraru, C., Amann, R., Hourdez, S., Girguis,
514 P.R., Wankel, S.D., Barbe, V., Pelletier, E., Fink, D., Borowski, C., Bach, W., Dubilier, N.,
515 2011. Hydrogen is an energy source for hydrothermal vent symbioses. *Nature* 476, 176–180.
- 516 Prosser, J.I., 2010. Replicate or lie. *Environ. Microbiol.* 12, 1806–1810.
- 517 Pruski, A.M., Fiala-Médioni, A., 2003. Stimulatory effect of sulphide on thiotaurine synthesis in
518 three hydrothermal-vent species from the East Pacific Rise. *J. Exp. Biol.* 206, 2923–2930.
- 519 R Development Core Team, 2013. R Development Core Team (2013). R: A language and
520 environment for statistical computing. R Foundation for Statistical Computing, Vienna,
521 Austria. ISBN 3-900051-07-0, URL <http://www.R-project.org>.
- 522 Riou, V., Duperron, S., Halary, S., Dehairs, F., Bouillon, S., Martins, I., Colaço, A., Serrão Santos,
523 R., 2010. Variation in physiological indicators in *Bathymodiolus azoricus* (Bivalvia:
524 Mytilidae) at the Menez Gwen Mid-Atlantic Ridge deep-sea hydrothermal vent site within a
525 year. *Mar. Environ. Res.* 70, 264–271.

- 526 Riou, V., Halary, S., Duperron, S., Bouillon, S., Elskens, M., Bettencourt, R., Santos, R.S., Dehairs,
527 F., Colaço, A., 2008. Influence of CH₄ and H₂S availability on symbiont distribution, carbon
528 assimilation and transfer in the dual symbiotic vent mussel *Bathymodiolus azoricus*.
529 Biogeosciences 5, 1681–1691.
- 530 Shillito, B., Gaill, F., Ravaux, J., 2014. The Ipcamp pressure incubator for deep-sea fauna. J. Mar.
531 Sci. Technol.-Taiwan 22, 97–102.
- 532 Shillito, B., Hamel, G., Duchi, C., Cottin, D., Sarrazin, J., Sarradin, P.-M., Ravaux, J., Gaill, F.,
533 2008. Live capture of megafauna from 2300 m depth, using a newly designed pressurized
534 recovery device. Deep Sea Res. I 55, 881–889.
- 535 Thurber, R.V., Willner-Hall, D., Rodriguez-Mueller, B., Desnues, C., Edwards, R.A., Angly, F.,
536 Dinsdale, E., Kelly, L., Rohwer, F., 2009. Metagenomic analysis of stressed coral
537 holobionts. Environ. Microbiol. 11, 2148–2163.
- 538 Trask, J.L., Van Dover, C.L., 1999. Site-specific and ontogenetic variations in nutrition of mussels
539 (*Bathymodiolus* sp.) from the Lucky Strike hydrothermal vent field, Mid-Atlantic Ridge.
540 Limnol. Oceanogr. 44, 334–343.
- 541 Van Dover, C., 2000. The ecology of deep-sea hydrothermal vents. Princeton University Press,
542 Princeton, N.J.
- 543 Van Dover, C.L., German, C.R., Speer, K.G., Parson, L.M., Vrijenhoek, R.C., 2002. Evolution and
544 biogeography of deep-sea vent and seep invertebrates. Science 295, 1253–1257.
- 545 Von Cosel, R., Cosel, R.V., Comtet, T., Krylova, E.M., 1999. *Bathymodiolus* (Bivalvia: Mytilidae)
546 from hydrothermal vents on the Azores Triple Junction and the Logatchev Hydrothermal
547 Field, Mid-Atlantic Ridge. Veliger 42, 218–248.
- 548 Von Cosel, R., Salas, C., Høisæter, T., 2001. Vesicomidae (Mollusca: Bivalvia) of the genera
549 *Vesicomya*, *Waisiuconcha*, *Isorropodon* and *Callogonia* in the eastern Atlantic and the
550 Mediterranean. Sarsia 86, 333–366.
- 551 Wallner, G., Amann, R., Beisker, W., 1993. Optimizing fluorescent in situ hybridization with rRNA-
552 targeted oligonucleotide probes for flow cytometric identification of microorganisms.
553 Cytometry 14, 136–143.
- 554 Wentrup, C., Wendeberg, A., Schimak, M., Borowski, C., Dubilier, N., 2014. Forever competent:
555 Deep-sea bivalves are colonized by their chemosynthetic symbionts throughout their
556 lifetime. Environ. Microbiol. 16, 3699–3713.

Table 1

Probe	Target	Sequence [5' → 3']	Cy3	Cy5	FITC	Channel colour	Reference
EUB_338	Eubacteria	GCTGCCTCCCGTAGGAGT	+	+	+	red	Amann <i>et al.</i> , 1990
Imed_M-138	MOX	ACCATGTTGTCCCCCACTAA	+	-	-	green	Duperron <i>et al.</i> , 2008
Bang_T-642	SOX	CCTATACTCTAGCTTGCCAG	-	+	-	blue	Duperron <i>et al.</i> , 2005
NON_338	negative control	ACTCCTACGGGAGGCAGC	+	+	-	-	Wallner <i>et al.</i> , 1993

Table 2

Site		Menez Gwen		Rainbow	
Point		MG2		France 5	
Depth		830 m		2270 m	
Position		37°50.669 N 31°31.156 W		36°13.766 N 33°54.117 W	
Recovery mode		BioBox	PERISCOP	BioBox	PERISCOP
Maintained pressure		0%	83.60%	0%	76.50%
Number of individuals		7	10	3	16
Shell length mm (min-		32-47	26.3-39	88-97	67-88.5
2D FISH	% MOX	47.2	44.6	56.3	57.5
	% SOX	52.8	55.4	43.7	42.5
	S.D.	5.4	5.1	6.6	7.6
3D FISH	% MOX	46.5	44.3	56.3	56.3
	% SOX	53.5	55.7	43.7	43.7
	S.D.	5.8	5.7	6.4	8.3
0 bacteriocyte	% MOX	48.1	47.5	56.3	55.6
	% SOX	51.9	52.5	43.7	44.4
	S.D.	3.8	4.2	4.6	6.3

Figure 1

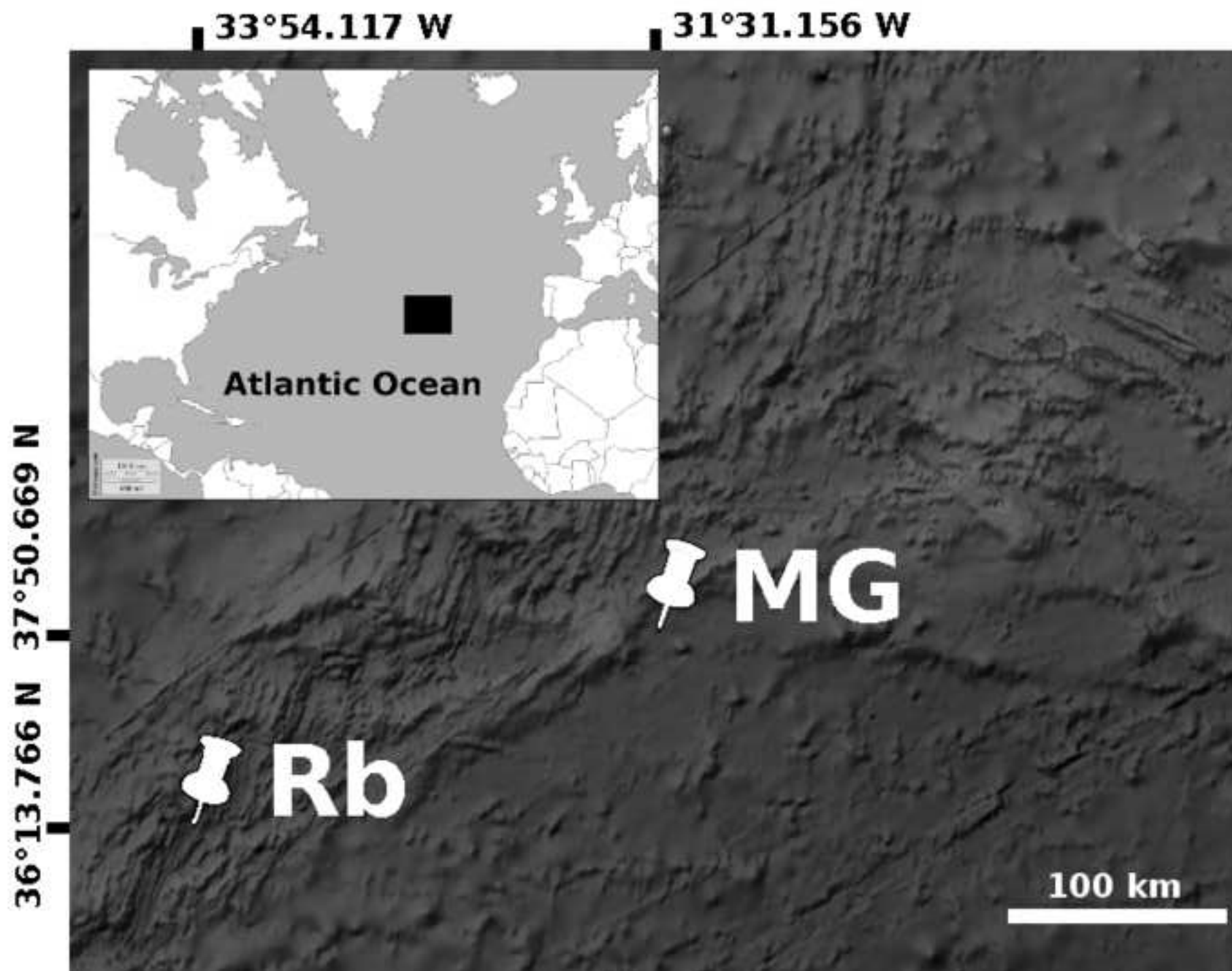


Figure 2A

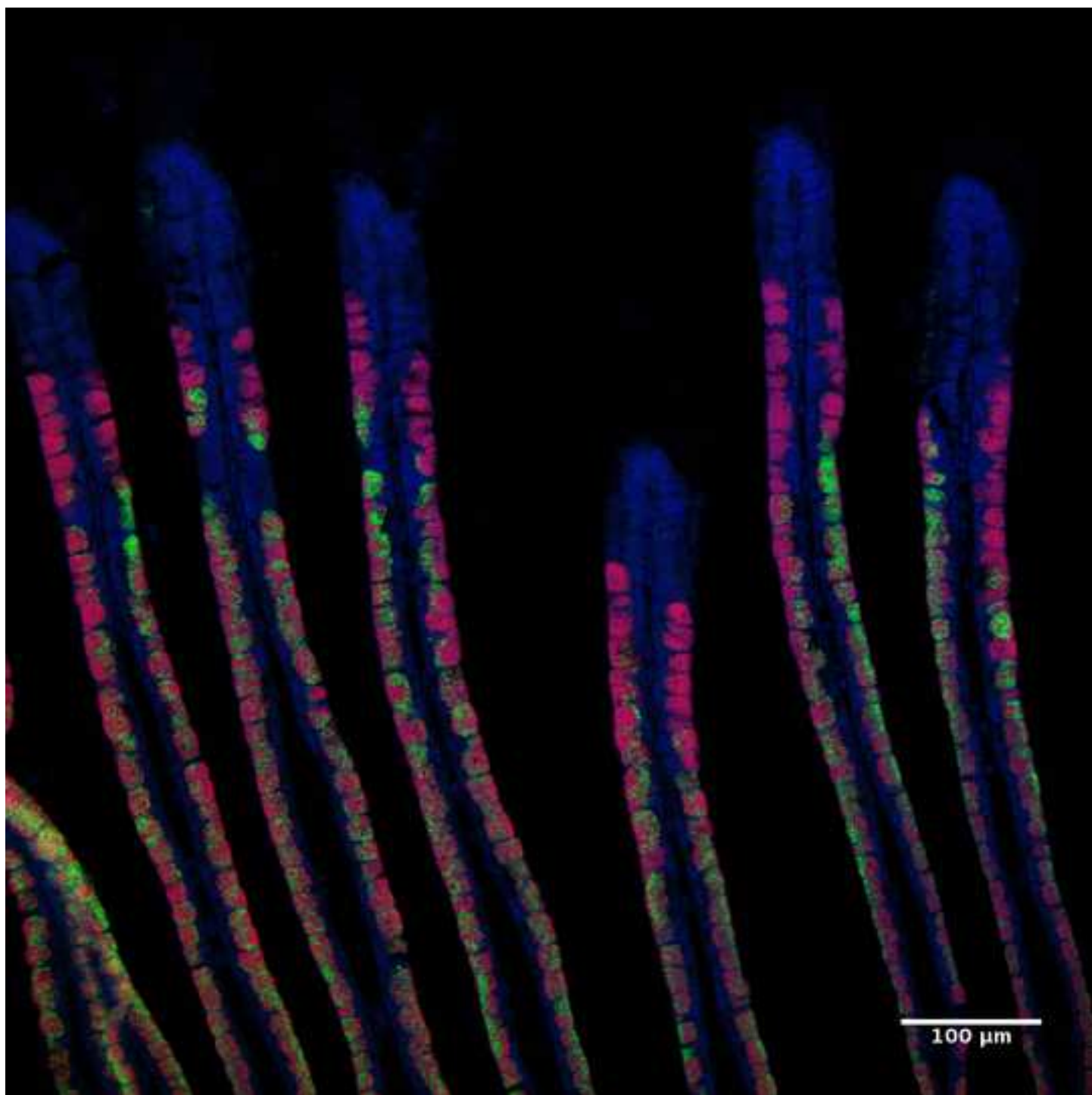


Figure 2B

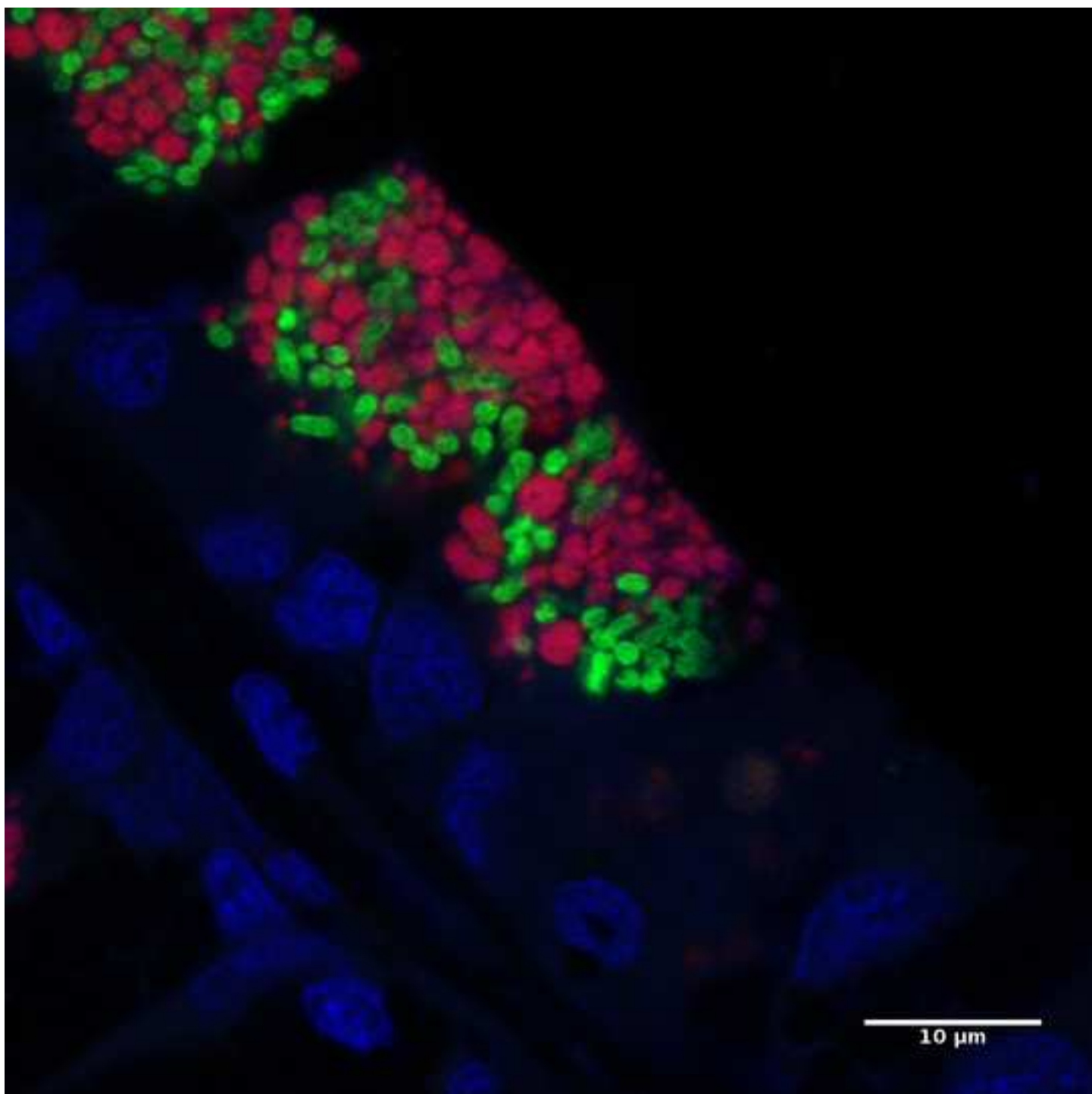


Figure 3

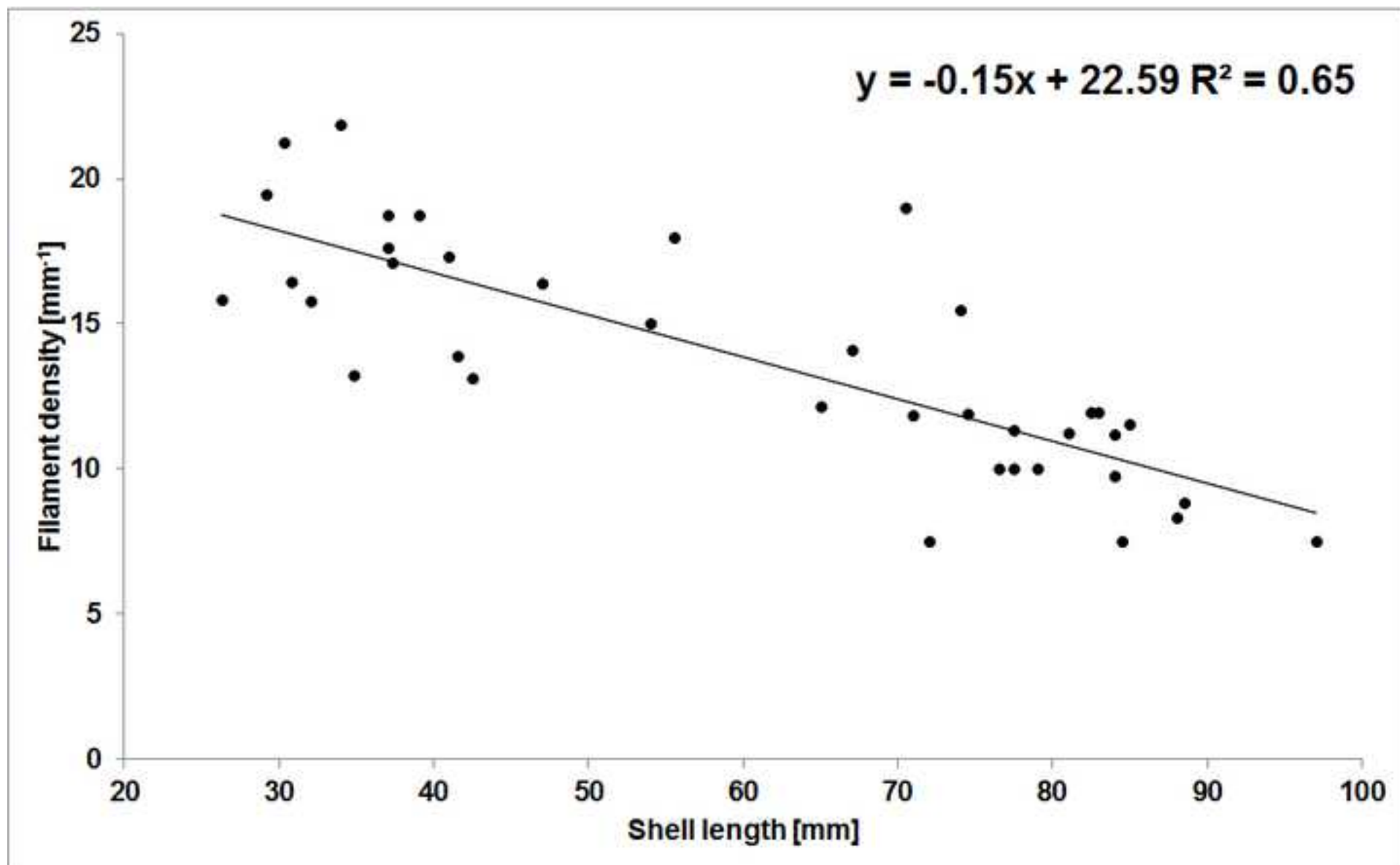


Figure 4

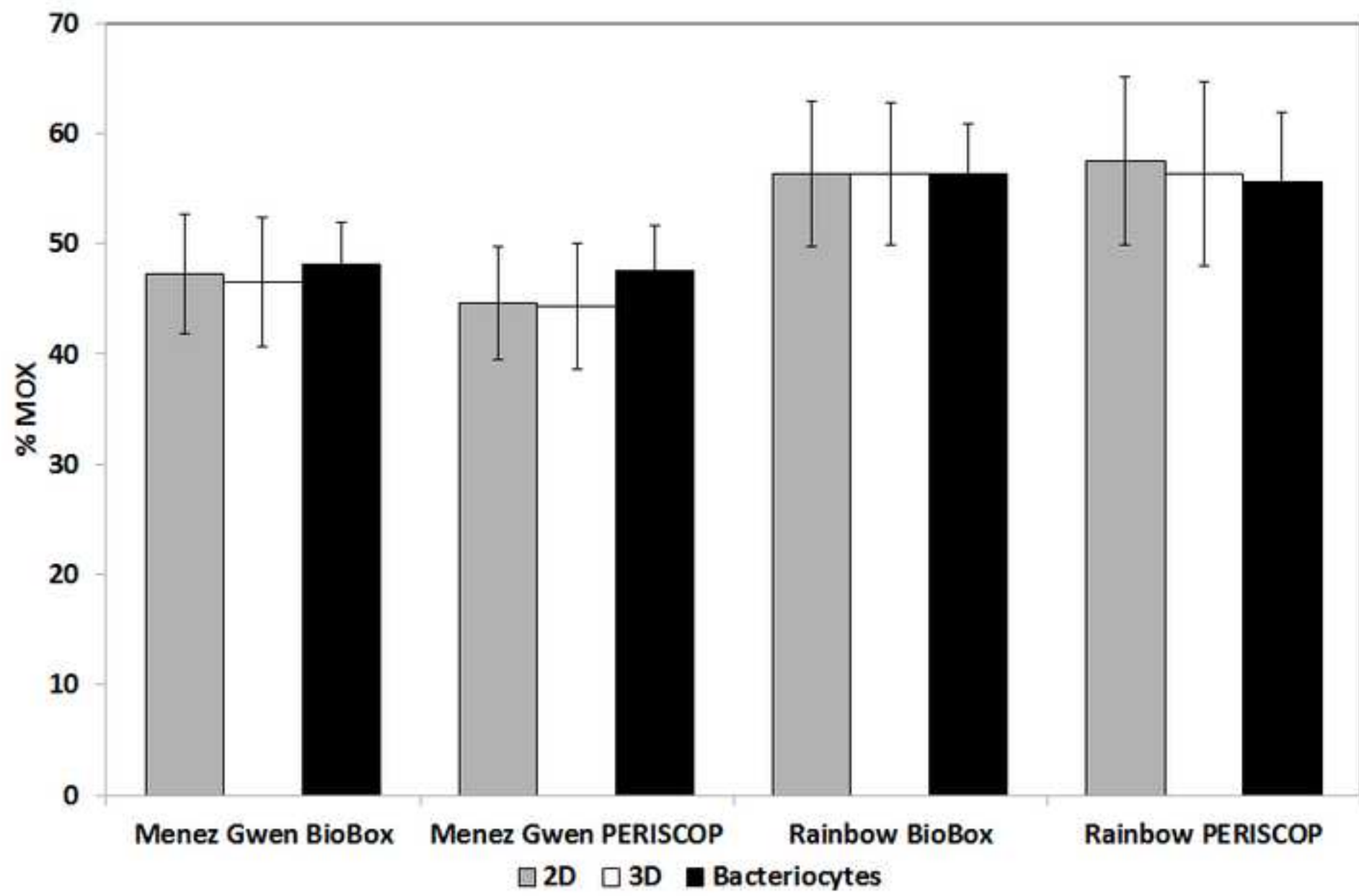


Figure 5

